

## THE CORROSION BEHAVIOUR OF DUPLEX STAINLESS STEEL IN CHLORIDE SOLUTIONS STUDIED BY XPS

### XPS RAZISKAVE KOROZIJSKEGA VEDENJA DUPLEKSNEGA NERJAVNEGA JEKLA V KLORIDNIH RAZTOPINAH

Aleksandra Kocijan, Črtomir Donik, Monika Jenko

Institute of metals and technology, Lepi pot 11, 1000 Ljubljana, Slovenia  
aleksandra.kocijan@imt.si

Prejem rokopisa – received: 2008-12-16; sprejem za objavo – accepted for publication: 2009-03-11

The evolution of the passive films formed on duplex stainless steel 2205 in a chloride solution was studied by X-ray photoelectron spectroscopy, and their compositions were analysed as a function of depth. The passive films on the duplex stainless steel contained the oxides of the two main elements, i.e., Fe and Cr. The alloying elements were found to improve the corrosion resistance of duplex stainless steels; however, their content within the passive layer was negligible. A strong chromium enrichment was observed in the passive layers with increasing chloride concentration. The potentiodynamic measurements were used to determine the corrosion behaviour of duplex stainless steel under different concentrations of chloride solution.

Keywords: duplex stainless steel, XPS, passive films

Z rentgensko fotoelektronsko spektroskopijo (XPS) smo raziskovali nastanek pasivne plasti na površini dupleksnega nerjavnega jekla 2205 v raztopini natrijevega klorida. Pasivna plast na površini tega jekla je vsebovala oksida dveh glavnih elementov Fe in Cr. Legirni elementi povečajo korozijsko odpornost dupleksnih nerjavnih jekel, njihova vsebnost v pasivni plasti pa je zanemarljiva. Z večanjem koncentracije kloridnih ionov se je močno povečala vsebnost kroma v pasivni plasti.

Ključne besede: dupleksno nerjavno jeklo, XPS, pasivne plasti

## 1 INTRODUCTION

Duplex stainless steels (DSSs) with a ferrite/austenite volume ratio of about 1:1 have been recognized as good corrosion-resistant materials in various aqueous environments<sup>1</sup>. The high Cr content together with the high Mo and N contents gives rise to a high pitting-corrosion resistance in chloride solutions. The presence of an approximately 50 % volume of ferrite results in an increase in the strength, as compared with the austenitic stainless steels<sup>2,3</sup>. It is generally known that DSS is also more resistant to stress corrosion cracking in chloride-containing solutions<sup>4</sup>. Molybdenum increases the stability of the passive film and, therefore, the ability of the stainless steel to resist the localised corrosion, including pitting and crevice corrosion, particularly in environments containing chloride ions<sup>4</sup>.

Various spectroscopic techniques have been used to study the corrosion behaviour of duplex stainless steels. Souto et al.<sup>5</sup> studied the passivation and the resistance to pitting corrosion of duplex stainless steel in neutral and alkaline buffered solutions, with and without chloride ions. The presence of NaCl enhanced the metal's electro-dissolution through the passive layer. The interpretation of the results was based on the presence of Cr and Ni in the alloy. Antony et al.<sup>6</sup> showed the aggressiveness of sulphate-reducing bacteria in a marine environment, which plays an important role in the corrosion of duplex

stainless steel. The initiation of the attack was evident from SEM and AFM studies. In addition, ESCA studies revealed that under anaerobic conditions sulphidation of the passive film occurs. Abreu et al.<sup>7</sup> pointed out the stabilising effect of molybdenum on the surface of the passive film, enhancing the formation of a layer on duplex stainless steel with a higher Cr/Fe ratio.

In the present work, 2205 duplex stainless steel was studied in various sodium chloride solutions. The composition and the depth profiles of the oxide films formed on 2205 duplex stainless steel at various potentials were studied by XPS analysis.

## 2 EXPERIMENTAL

Duplex 2205 stainless steel was investigated. Its composition was confirmed by analytical chemical methods, as shown in Table 1. The experiments were carried out in 0.9 %, 2 % and 3.5 % solutions of sodium chloride. All the chemicals were from Merck, Darmstadt, Germany. The test specimens were cut into discs of 15 mm diameter. The specimens were polished with SiC emery paper down to 1000 grit prior to the electrochemical studies, and to 4000 grit prior to the XPS studies, and then rinsed with distilled water. The specimens were then embedded in a Teflon PAR holder and employed as the working electrode. The reference electrode was a

saturated calomel electrode (SCE, 0.242 V vs. SHE) and the counter electrode was a high-purity graphite rod.

**Table 1:** The composition of the 2205 duplex stainless steel (w/w)  
**Tabela 1:** Sestava dupleksnega nerjavnega jekla 2205 (w/w)

Material	Cr	Ni	Mn	Si	P	S	C	Mo
duplex 2205	22.74	5.74	1.37	0.38	0.032	0.001	0.03	2.57

The potentiodynamic measurements were recorded using an EG&G PAR PC-controlled potentiostat/galvanostat Model 263 with M252 and Softcorr computer programs. The specimens were immersed in the solution 1 h prior to the measurement in order to stabilize the surface at the open-circuit potential. The potentiodynamic curves were recorded, starting at 250 mV more negative than the open-circuit potential. The potential was then increased, using a scan rate of 1 mV s<sup>-1</sup>, until the transpassive region was reached.

The passive layers on the alloy's surface were formed under potentiostatic conditions for 1 hour at potentials of -0.2 V, 0.4 V, 0.8 V and 1.2 V vs. SCE. These potentials were chosen with reference to the characteristic features of the polarization curve (see **Figure 1**). After the electrochemical preparation, the specimens were rinsed with distilled water, dried and transferred to the analyzer chamber within an hour.

The XPS measurements were performed using a VG Scientific Microlab 310F instrument, non-monochromatized Mg K<sub>a</sub> radiation ( $E = 1253.6$  eV) and a hemispherical electron analyzer operating at a pass energy of 20 eV. The spectra were collected using Avantage 3.41V data-analysis software, supplied by the manufacturer. The thickness of the passive layer was determined by argon-ion sputtering for different time intervals. The reference sputtering rate was 0.01 nm/s, and this was calculated relative to Ta<sub>2</sub>O<sub>5</sub> as the intensity of the oxygen signal decreased to a half. Sputter depth profiles were measured for the passive films formed at two selected potentials, -0.2 V and 1.2 V, in all three test solutions containing a different concentration of NaCl.

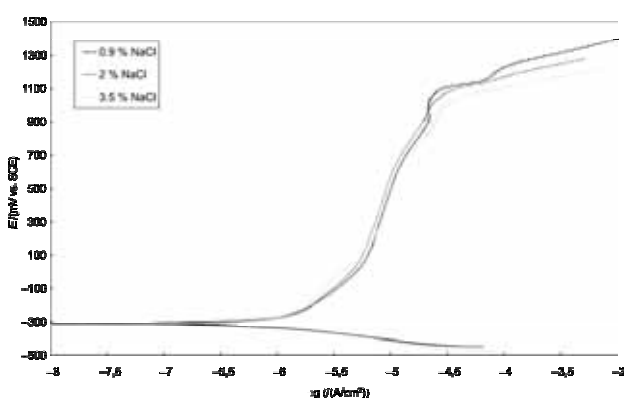


**Figure 1:** Polarisation curves recorded for the 2205 duplex stainless steel in chloride solutions with three different concentrations

**Slika 1:** Polarizacijske krivulje dupleksnega nerjavnega jekla 2205 v raztopinah natrijevega klorida z različnimi koncentracijami

After a background subtraction, according to Shirley 10, and processing with CasaXPS software developed by Fairley 11, the XPS signals were separated into the contributions from the different species. The spectra were evaluated using the parameters of standard peaks.

**Figure 2** presents examples of the deconvoluted spectra. To calculate the composition of the passive layer the peak areas were corrected with the corresponding photo-ionization cross-sections:  $\sigma(\text{Fe } 2p_{3/2}) = 9.68$ ,  $\sigma(\text{Cr } 2p_{3/2}) = 6.90$ ,  $\sigma(\text{Mo } 3d_{5/2}) = 5.62$ ,  $\sigma(\text{Ni } 2p_{3/2}) = 13.04$ , and  $\sigma(\text{O } 1s) = 2.51$  12, 13.

### 3 RESULTS

**Figure 1** shows the potentiodynamic curves for 2205 DSS in mass fractions 0.9 %, 2.0 % and 3.5 % of sodium chloride solutions. After 1 h of stabilization at the open-circuit potential, the corrosion potential ( $E_{\text{corr}}$ ) for the 2205 DSS in all three solutions was approximately -0.300 V. Following the Tafel region, the alloy exhibited passive behaviour. The extent of the passive range slightly decreased with the increasing chloride concentration. The passive range is limited by the breakdown potential ( $E_b$ ), which corresponds to the oxidation of water and the transpassive oxidation of metal species. The breakdown potential for the 2205 DSS in a 0.9 %

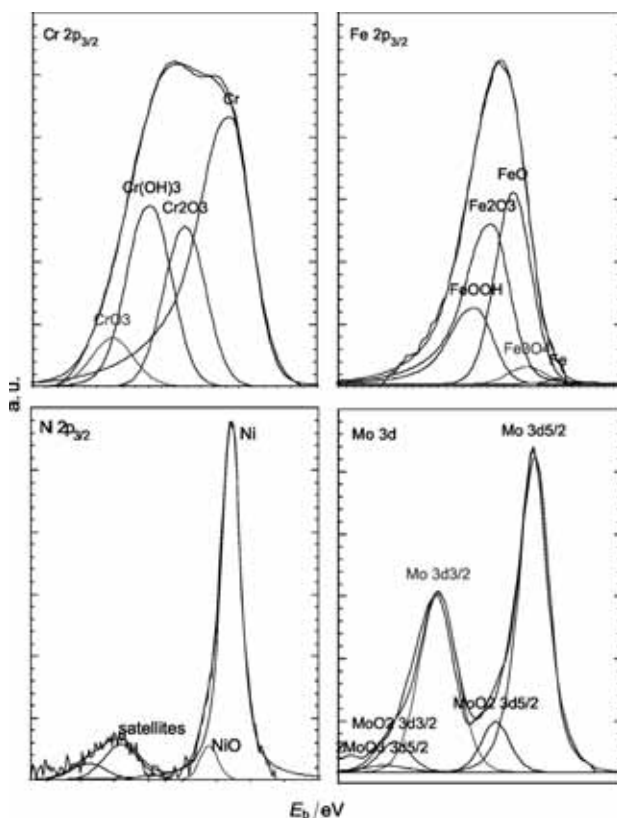


**Figure 2:** Examples of fitted Cr 2p<sub>3/2</sub>, Fe 2p<sub>3/2</sub>, Ni 2p<sub>3/2</sub> and Mo 3d XPS-spectra

**Slika 2:** Primeri obdelanih Cr 2p<sub>3/2</sub>, Fe 2p<sub>3/2</sub>, Ni 2p<sub>3/2</sub> and Mo 3d XPS-spektrov

chloride solution was approximately 1.10 V, and this moved towards more negative values with an increasing chloride concentration, i.e., to 1.03 V and 1.00 V, respectively.

The XPS spectra were recorded after exposures at potentials of special interest, in close correlation to the polarization curves. The samples were oxidised at the selected potentials prior to the XPS measurements for 30 min.

**Figure 3** presents the cationic fractions of the passive layer after the oxidation of the 2205 DSS in the presence of three different chloride solutions. The bulk composition of the alloy is indicated by the dotted lines, so

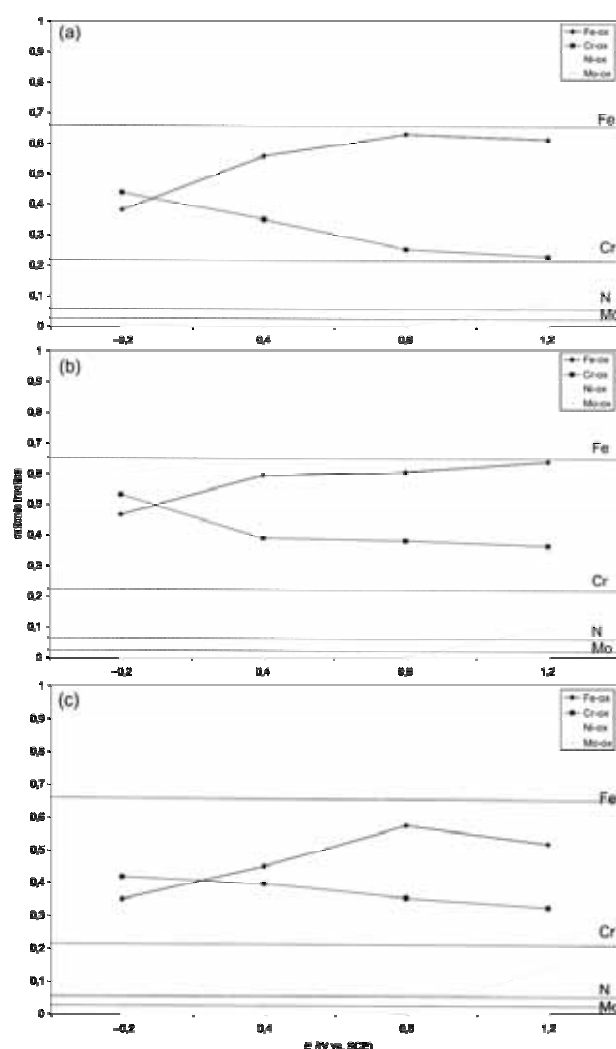


**Figure 3:** Cationic fractions of the passive layer on the 2205 duplex stainless steel in (a) 0.9 % NaCl, (b) 2 % NaCl and (c) 3.5 % NaCl as a function of the oxidation potential. The dashed lines denote the bulk values of the atomic fractions for Fe, Cr, Ni and Mo within the alloy. The oxidation time was 30 min.

**Slika 3:** Kationske frakcije površine pasivne plasti na dupleksnem nerjavnem jeklu 2205 v raztopinah natrijevega klorida z različnimi koncentracijami (a) 0,9 % NaCl, (b) 2 % NaCl and (c) 3,5 % NaCl v odvisnosti od potenciala oksidacije. Črtkane črte prikazujujo vrednosti atomskih frakcij Fe, Cr, Ni in Mo v osnovnem materialu. Čas oksidacije je 30 min.

that the relative enrichment and depletion of the particular elements are clearer. In all three solutions the fraction of Fe was less than that of the bulk concentration, and this effect increased with the chloride concentration. The passive layer was Cr-enriched compared to the bulk concentration; the Cr concentration was somewhat higher at lower potentials and slightly decreased at higher anodic potentials. The concentration of the Ni was strongly reduced compared to the bulk concentration; that of the Mo was slightly increased at higher anodic potentials compared to the bulk concentration. This result suggests the preferential dissolution of Fe and Ni from the passive layer in the presence of chloride ions.

**Figures 4 and 5** show the composition depth profiles for the 2205 DSS after the oxidation at -0.2 V and 1.2 V in the presence of three different chloride solutions. The profiles present the relative concentrations of the

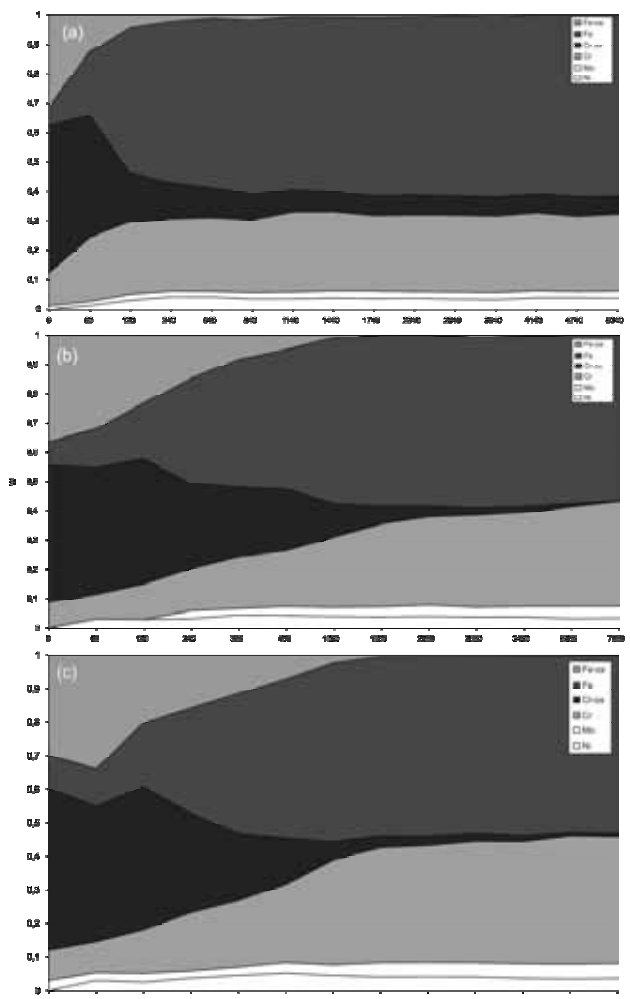


**Figure 4:** Depth profiles of the 2205 duplex stainless steel as a function of sputtering time after oxidation at -0.2 V in (a) 0.9 % NaCl, (b) 2 % NaCl and (c) 3.5 % NaCl

**Slika 4:** Globinski profili dupleksnega nerjavnega jekla 2205 v odvisnosti od časa jedkanja po oksidaciji pri -0,2 V (a) 0,9 % NaCl, (b) 2 % NaCl in (c) 3,5 % NaCl

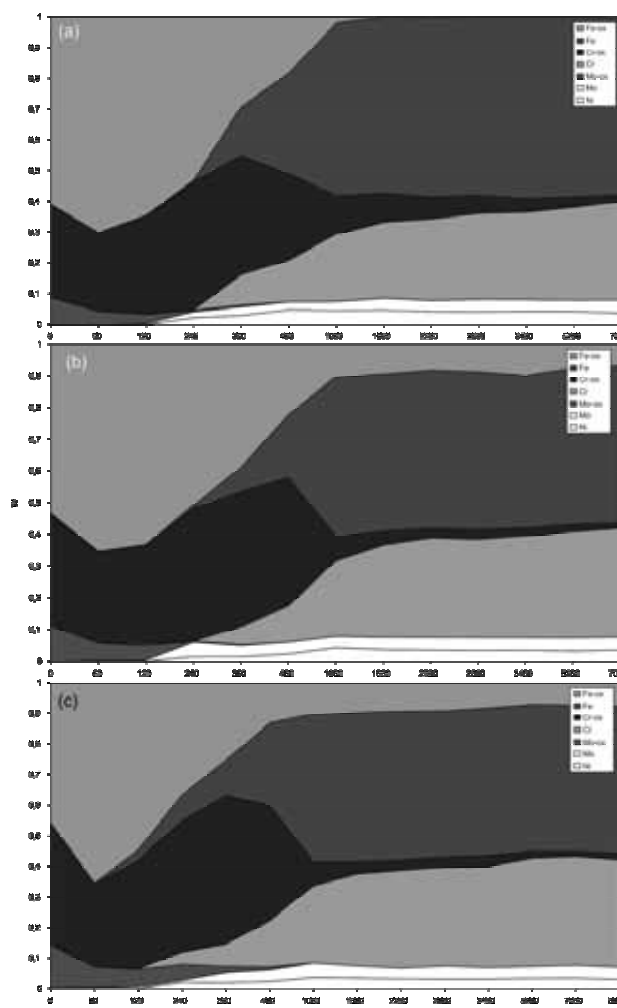


**Figure 5:** Depth profiles of the 2205 duplex stainless steel as a function of sputtering time after oxidation at 1.2 V in (a) 0.9 % NaCl, (b) 2 % NaCl and (c) 3.5 % NaCl

**Slika 5:** Globinski profili dupleksnega nerjavnega jekla 2205 v odvisnosti od časa jedkanja po oksidaciji pri 1,2 V v (a) 0,9 % NaCl, (b) 2 % NaCl and (c) 3,5 % NaCl

metallic and oxidised species of a particular metal. After each sputtering step the composition of each oxide and metal species was plotted cumulatively along the ordinate, so that the total composition amounted to 100 %. The precise stoichiometry of the oxide cannot be determined due to ion-sputtering-induced effects, such as the reduction of the oxidation state<sup>16,17</sup>. The films were seen to exhibit a gradual oxide-to-metal transition, with complete oxidation only at the outermost surface. Nevertheless, the metallic parts of the individual components appeared at the surface due to a less uniform oxidation or an effect related to ion-sputtering reduction<sup>16,17</sup>.

The main constituent of the passive layer formed at the surface of the 2205 DSS after oxidation at -0.2 V in all three solutions was Cr-oxide, and the total amount of Cr was enriched compared to the bulk concentration (**Figure 4**). The second major constituent of the passive layer was Fe-oxide, although the total amount of Fe was

lower than in the bulk. The amounts of Mo- and Ni-oxides were very low, especially for the Ni, in comparison to the bulk.

After the oxidation at 1.2 V the passive layer consisted predominantly of Fe-oxides and was slightly depleted in Cr-oxide (**Figure 5**), compared to the results at -0.2 V, due to the effects explained later. The amount of Ni species was significantly depleted at the outer layers. With the increasing chloride concentration the amounts of Fe and Ni species decreased due to the preferential dissolution in the presence of chloride ions. Therefore, the amount of Cr-oxide increased.

#### 4 DISCUSSION

The corrosion-passivation processes of a duplex stainless steel polarised in neutral chloride solutions were investigated by using electrochemical and surface analytical techniques. The results obtained in the present work reveal that the passive film formed on the surface of the DSS 2205 in the chloride solution at pH 7 contains oxides of the two main elements, i.e., Fe and Cr. The oxides of the alloying elements Ni and Mo are negligible compared to the bulk, except for the increased Mo concentration in the transpassive region. Previous studies have confirmed that for stainless steels the amount of nickel present in the passive film is very small<sup>18,8,19</sup>. Abreu et al.<sup>8</sup> also observed only a small amount of Ni distributed along a passive film of DSS. Milošev et al.<sup>18</sup> reported the strong depletion of Ni in the layer formed on AISI 316L in a neutral solution compared to the bulk content. Clayton et al.<sup>19</sup> emphasized that Ni is rarely observed in the passive films of stainless steels formed in solutions containing chloride ions. From the equilibrium diagrams it is expected that at potentials anodic to 0 V, chromium would dissolve preferentially in the buffer solution<sup>14</sup>. The XPS results confirm this prediction: when the DSS is passivated at potentials = 0 V, the chromium level slightly decreases and that of the iron increases towards the oxide-solution interface (**Figure 5**).

Increasing the chloride concentration causes a substantial reduction in the potential range for passivity and further growth of the oxide film is hindered as the metal electro-dissolution becomes the dominant electrochemical process<sup>3</sup>. The passivity of stainless steels arises from the high corrosion resistance exhibited by the Cr(III) oxide-hydroxides present in the passivating layers. The role of the alloyed chromium in enhancing the passivity of stainless steels is frequently explained in terms of a percolation model of passivation<sup>3</sup>. It is considered that chromium forms insoluble Cr<sub>2</sub>O<sub>3</sub>, and a continuous network of Cr-O-Cr-O is then produced, which prevents the dissolution of iron.

The addition of nickel has a beneficial influence on the corrosion resistance of ferritic steels<sup>3</sup>. However, its influence is less effective than in the case of chromium,

since Ni(II) ions do not anchor the water molecules and the hydroxyl ions enough to prevent the chloride ions from migrating through the passivating layer by replacing the water and hydroxyl groups, and therefore, cause localised corrosion.

Molybdenum does not significantly change the composition of the film, but its presence is believed to contribute to the deprotonation of the hydroxide by acting as an electron acceptor, creating an oxygen abundance in the inner regions of the passive layer and helping in the formation of a stable  $\text{CrO}_3/\text{Cr}_2\text{O}_3$  protecting oxide. The other effect of this reaction is the production of protons; they will be drawn towards the solution by the cation-selective properties of the outer layer. This will increase the proton activity on the surface and assist in the formation of ammonium ions. This is, according to Olsson<sup>20</sup>, one of the conceivable mechanisms of synergism between molybdenum and nitrogen in the DSS. Clayton and Martin emphasised that nitrogen reactions, particularly at higher potentials, are extremely sluggish, and that there is a possibility for the formation of soluble oxidised species, which may be dispersed in the solution and not observed in the surface analyses<sup>21</sup>. Our results agree with this assertion, since the concentration of Mo in the passive layer was strongly diminished compared to the bulk and N was not detected at all. However, this induced modification in the film can explain the high Cr/Fe ratio measured in the XPS depth profiles, which indicates the better corrosion characteristics of molybdenum-containing alloys.

## 5 CONCLUSIONS

The chemical composition of the film formed on duplex stainless steel showed the presence of two main oxides, i.e., Fe and Cr. The oxides of the alloying elements Ni and Mo were negligible compared to the bulk. A slight decrease of the chromium content close to the oxide/solution interface at higher anodic potentials was also observed. The compositional changes in the passive film can be explained on the basis of the

selective solubility of the oxides at the applied potentials. Molybdenum mainly enhances the effect of other passivating species, i.e., Cr, more than acting directly in the passivating process in chloride media since its content in the oxide layer is minor.

## 6 REFERENCES

- <sup>1</sup>S. T. Tsai, K. P. Yen, H. C. Shih, *Corros. Sci.*, 40 (1998), 281–295
- <sup>2</sup>F. Tehovnik, F. Vodopivec, L. Kosec, M. Godec, *Mat. Tech.*, 40 (2006), 129–138
- <sup>3</sup>A. Kocijan, Č. Donik, M. Jenko, *Corros. sci.*, 49 (2007), 2083–2098
- <sup>4</sup>J. A. Platt, A. Guzman, A. Zuccari, D. W. Thornburg, B. F. Rhodes, Y. Ossida, D. W. Thornburg, B. F. Rhodes, Y. Ossida, B. K. Moore, *American Journal of Orthodontics and Dentofacial Orthopedics*, 112 (1997), 69–79
- <sup>5</sup>R. M. Souto, I. C. Mirza Rosca, S. Gonzales, *Corrosion*, 57 (2001), 300–306
- <sup>6</sup>P. J. Antony, S. Chongdar, P. Kumar, R. Raman, *Electrochim. Acta* 52 (2007), 3985–3994
- <sup>7</sup>C. M. Abreu, M. J. Cristóbal, R. Losada, X. R. Nóbrega, G. Pena, M. C. Pérez, *Electrochim. Acta* 49 (2004), 3049–3056
- <sup>8</sup>K. Hashimoto, K. Asami, *Corros. Sci.* 19 (1979) 3, 251–260
- <sup>9</sup>D. A. Shirley, High-resolution X-ray photoemission spectrum of valence bands of gold, *Phys. Rev. B5* (1972), 4709
- <sup>10</sup>N. Fairley, CasaXPS VAMAS Processing Software, <http://www.casaxps.com/>
- <sup>11</sup>J. H. Scofield, *J. Electron Spectrosc. Relat. Phenom.* 8 (1976), 129–137
- <sup>12</sup>R. F. Reilman, A. Msezane, S. T. Manson, *J. Electron Spectrosc. Relat. Phenom.* 8 (1976), 389–394
- <sup>13</sup>N. Ramasubramanian, N. Preocanin, R. D. Davidson, *J. Electrochem. Soc.* 132 (1985), 793–798
- <sup>14</sup>P. Delahay, *New instrumental methods in electrochemistry* Interscience, New York, London, 1954, 115–145
- <sup>15</sup>W. H. Hocking, F. W. Stanchell, E. McAlpine and D. H. Lister, *Corros. Sci.* 25 (1985), 531–557
- <sup>16</sup>N. S. McIntyre, D. G. Zetaruk, E. V. Murphy, *Surf. Interface Anal.* 1 (1979) 105–110
- <sup>17</sup>I. Milošev, H.-H. Strehblow, *J. Biomed. Res.* 52 (2000) 2, 404–412
- <sup>18</sup>C. R. Clayton, Y. C. Lu, *J. Electrochem. Soc.* 133 (1986) 2465–2472
- <sup>19</sup>C. A. Olsson, *Corros. Sci.* 37 (1995) 467–479
- <sup>20</sup>C. R. Clayton, K. G. Martin, in *Proc. High Nitrogen Steels-HNS 88*, The Institute of Metals, London (1988) p. 256